
179th Meeting of the Acoustical Society of America

Acoustics Virtually Everywhere

7-11 December 2020

Underwater Acoustics: Paper 2aUWa2

Vector Sensor Beam Steering for Underwater Acoustic Communications

Fabrizio de Abreu Bozzi

*Laboratory of Robotics and Engineering Systems (LARSys), University of Algarve, Faro, 8000-218,
PORTUGAL; fabricioboizzi@gmail.com*

Sergio M. Jesus

*Laboratory of Robotics and Engineering Systems (LARSys), University of Algarve, Faro, 8005-139,
PORTUGAL; sjesus@ualg.pt*

Acoustic Vector Sensors (VS) have been widely used for direction-of-arrival estimation in the past, while the employment of VS for underwater communications is a recent topic. Due to its compact size, VS may be used as a receiver in applications such as on board of Unmanned Underwater Vehicles (UUV), providing higher maneuverability and operational capabilities. Thus, in this study, the communication performance of a VS beam-steering technique is quantified. The performance analysis is made comparing the VS beam-steering with the VS time-reversal method in a shallow water simulation. The underwater channel is given by the seismo-acoustic propagation model, OASES. A Phase Shift Keying (PSK) modulation is adopted and the receiver includes a Decision Feedback Equalizer. An individual analysis of horizontal and vertical particle velocity is made to show the steering effects in the error performance. Moreover, as the steering angle is range-dependent, a comparison between methods is performed varying the range. The result indicates that the optimum steering angle, which brings less error, may not be related to the source direction. Furthermore, the proposed receiver shows the outperformance comparing to the time-reversal in both SNR and range, demonstrating the spatial filter advantage provided by this co-located sensor.

1. INTRODUCTION

Underwater acoustic systems have employed compact, autonomous, low cost, and efficient tools. Autonomous Underwater Vehicles (AUV) is an example of a tool used for several ocean exploration tasks. An AUV usually carries one acoustic modem on-board, linking the AUV to the surface-control or other AUV in network. In this sense, underwater communications provide flexibility in operations (do not need cables), real-time monitoring, on-the-fly objective changes, and may reduce the autonomous control complexity.

Underwater acoustic communication (UWAC) issues, such as the limited bandwidth, severe fading, and inter-symbol interference caused by multipath have been widely studied.¹ The use of hydrophone arrays is an effective solution that explores the array gain or spatial diversity. However, this solution may not be suitable for small platforms such as AUV or underwater station, due to their size, weight, and autonomy restrictions.

Acoustic vector sensors (VS) are a compact option that has been tested as receiver for UWAC.² Vector sensors are devices that measure pressure and particle motion information (usually velocity) in a co-located sensor. Particle velocity can be obtained by pressure-gradient or inertial sensors. The former uses two hydrophones to estimate the particle velocity, and the latter uses an inertial mass that responds directly to the particle motion, velocity, or acceleration.^{3,4} Particle velocity provides directional information, and methods attempt to take advantage of this inherent directionality to enhance communications performance.

Thus, this study uses one vector sensor as a receiver in a point-to-point communication system. While vector sensors have been widely used for sonar applications,⁵ the available literature is relatively recent for communications. Most studies aim to compare VS to pressure-only arrays, which reinforce VS usability.² However, there is a lack of studies comparing VS methods and its spatial filtering capability is not fully explored. In this regard, the present work quantifies the performance of two VS methods in a case study simulation. The first method, called VS beam steering, uses the particle velocity channels to focus the receiver to an optimum direction, acting as beamforming. For this method, an individual channel analysis is proposed to quantify the impact of each particle velocity component on the performance. The second method, named VS passive time-reversal, is based on the passive time-reversal method, except that the input signals are the pressure-equivalent particle velocity. A comparative analysis between the receivers uses coherent modulation Phase Shift-Keying (PSK). Furthermore, the communication performance is also quantified varying the receiver along the range.

2. VECTOR SENSORS AS A RECEIVER FOR COMMUNICATIONS

This section presents two methods that use particle velocity channels to enhance communications' performance. Since the particle velocity components are combined to the pressure channel, they are usually converted to a pressure-equivalent. Thus, the particle velocity physics and the relation with pressure is also demonstrated.

A. PARTICLE VELOCITY

In acoustics, particles (displacement, velocity, or acceleration) may be defined in terms of continuum mechanics.⁶ The size of a particle is not a fixed value, but it is considered large enough to represent a continuous volume and small enough to not affect the acoustic parameters in a volume. Considering a homogeneous, isotropic, and non-viscous medium, the particles move around an equilibrium point. A fundamental acoustic equation is given by Euler's equation or equation of particle motion:

$$\nabla p = -\rho_0 \frac{\partial \mathbf{v}}{\partial t} = -j\omega \rho_0 \mathbf{v}, \quad (1)$$

where ∇ is the gradient operator, p is the pressure, ρ_0 is the medium static density, \mathbf{v} is the particle velocity vector, and t is the time. The minus sign means that the reference is pointing to source (opposite to the wave propagation). Note that each pressure gradient component is proportional to the acoustic acceleration. Additionally, a practical relation is presented on the right-hand side, for the harmonic time dependence in angular frequency ω .

A complete solution for the acoustic field is $p = p_0 e^{j(\omega t \pm kr)}$, being p_0 the reference pressure, the wave vector $\mathbf{k}^2 = k_x^2 + k_y^2 + k_z^2$, and r the distance. Solving Eq. 1 in pressure leads to:

$$\mathbf{v} = -\frac{1}{j\omega\rho_0}\nabla p = -\frac{1}{\rho_0 c}\left(1 - \frac{j}{kr}\right)p, \quad (2)$$

where there is a phase difference between pressure and particle velocity. Note that for small values of kr (near-field, $kr \ll 1$) means that pressure and velocity have 90° in phase difference. On the other hand, if kr is considered large ($kr \gg 1$), then velocity and pressure are nearly in phase. Thus, under this last restrictive condition (for plane-waves),

$$p = -\rho_0 c \mathbf{v}, \quad (3)$$

where the product $\rho_0 c$ is the acoustic impedance. This equation provides the pressure-equivalent particle velocity. Moreover, Eq. 3 is useful for combining pressure and velocity channels to the same unity. Hereafter, readers may notice that particle velocity will also refer to pressure-equivalent particle velocity.

B. DATA MODEL

For a simplified two-dimensional (2D) depth-range underwater scenario, the input-output relation is given by:

$$\begin{aligned} p &= h \otimes s + n, \\ p_{vx} &= h_{vx} \otimes s + n_{vx}, \\ p_{vz} &= h_{vz} \otimes s + n_{vz}, \end{aligned} \quad (4)$$

where s represents the transmitted signal, $h/h_{v(x/z)}$ represent the channels (given by the OASES model⁷), and $p/p_{v(x/z)}$ are the pressure/pressure-equivalent (the index x , and z stands for horizontal and vertical particle velocities). In Eq. 4, \otimes stands for convolution in time, and n is the additive noise. The signal and the noise are assumed to be uncorrelated in time and space. If the noise is azimuthally isotropic and it has spherical symmetry, both horizontal and vertical noises are uncorrelated with the other noise terms.⁸ In this assumption, the noise power at the pressure channel is equal to the noise power of the pressure-equivalent velocity components.² It is known that VS based on pressure-gradient or accelerometers measurements may present distinct noise sensitivity.⁹ However, this work will not consider the VS technological characteristic and the results can be used for both types of sensors.

C. COMMUNICATIONS SYSTEM USING VECTOR SENSORS

The increased understanding on underwater channel physics, including advances in acoustic simulation models, and field experiments has suggested adaptive methods and new equalization techniques to improve the communication transmission rate. Experimental results have shown the possibility of using phase-coherent modulation, which takes advantage of an efficient bandwidth usage.¹⁰ Thus, the present work uses a Phase Shift-Keying (PSK) modulation and a Decision Feedback Equalizer (DFE).

Passive time-reversal followed by a single DFE is one method that is adapted to a VS.¹¹ Time-reversal mirror (or phase conjugation, when performed in frequency) uses the reciprocity propriety of sound propagation.¹² The basic idea is to play back, in time-reversed, the received signals on the pressure-only array.

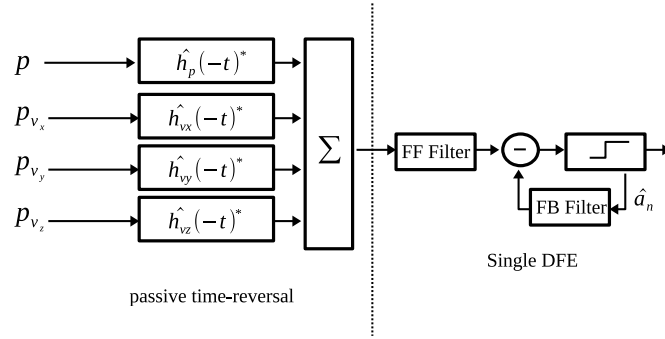


Figure 1: VS passive time-reversal.

The result is a retro-focusing to the source, which causes Signal-to-Noise Ratio (SNR) improvement and Inter Symbol Interference (ISI) mitigation. The passive version (passive time-reversal) performs a similar operation, although the reverse transmission is performed synthetically (by software or hardware), which requires channel estimation. Figure 1 shows the called VS passive time-reversal method.

In Fig. 1, $p/p_{v(x/y/z)}$ are the VS output, $\hat{h}/\hat{h}_{v(x/y/z)}$ are the estimated channels, which are assumed to be known ($\hat{h}_{vy} = 0$ due to 2D simulation). The VS passive time-reversal output is given by:

$$y(t) = \sum_{m=1}^{M=4} h_m^*(-t)p_m(t), \quad (5)$$

where m is the number of channels. The VS passive time-reversal output is the input of a single DFE. One can say that an additional time-reversal advantage is to reduce the number of DFEs.¹¹ The DFE equalizer used in this work is composed of a feed-forward filter, a detector, and a feedback filter. The feed-forward filter is a fractional spaced delay with $\tau = T/2$ and the feedback is symbol-spaced. The adaptive metric is performed by the Minimum Square Error (MSE) criterion.¹³

The VS passive time-reversal receiver takes advantage of the particle velocity directional information, which provides diversity among VS channels. This diversity can be quantified by the low correlation values among channels, justifying the outperformance when comparing a VS to a pressure-only array. However, another possibility is weighting the particle velocity components, which is equivalent to steer the VS angle. This signal processing, called VS beam steering, performs the pressure and particle velocity combination in azimuth θ_0 and elevation ϕ_0 . In the frequency domain, it is represented as:⁴

$$\begin{aligned} \tilde{P}(\omega, \theta_0, \phi_0) &= P(\omega) + V_x(\omega) \cos(\theta_0) \cos(\phi_0) + V_y(\omega) \sin(\theta_0) \cos(\phi_0) + V_z(\omega) \sin(\phi_0), \text{ or} \\ \tilde{P}(\omega, 0, \phi_0) &= P(\omega) + V_x(\omega) \cos(\phi_0) + V_z(\omega) \sin(\phi_0) \Rightarrow 2D, \end{aligned} \quad (6)$$

where the $V_{x/y/z}$ are the pressure-equivalent particle velocity. Steering the angle means to focus in a direction and filter the unwanted interference. The procedure presented in Eq. 6 is simple and straightforward. Figure 2a shows the VS beam steering method. Note that the VS beam steering receiver replaces the channel estimation of the passive time-reversal for the weighted combined signal given by Eq. 6. Figure 2b shows a 2D radiation diagram steering the VS at $\phi_0 = 60^\circ$.

3. SIMULATIONS

The simulation is based on the Makai experiment scenario (MakaiEx). This experiment was a two week sea trial, which took place off the coast of Kauai Island, Hawaii, in 2005. A vector sensor array (VSA)

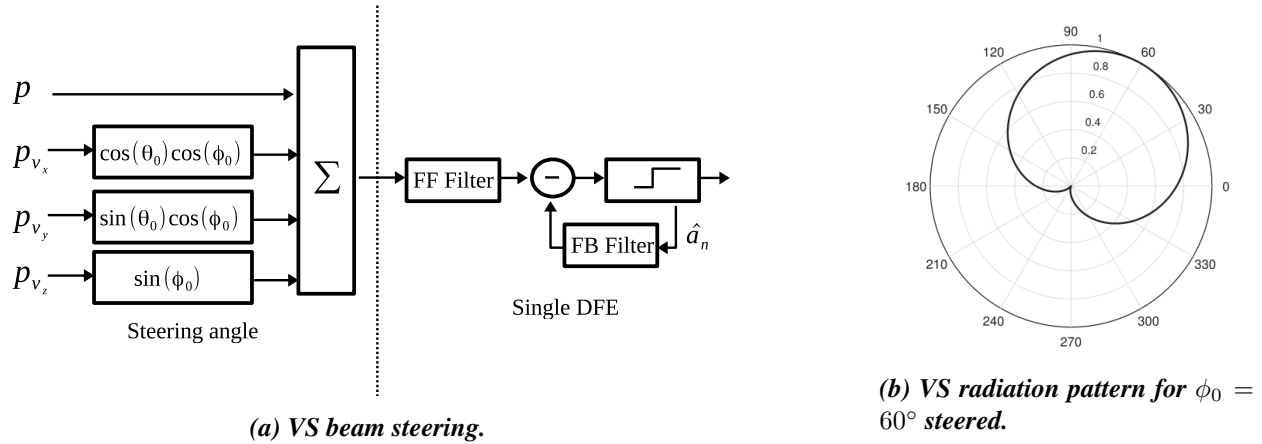


Figure 2: Vector sensor beam steering receiver.

was deployed at sea receiving different types of signals.¹⁴ In summary, each VS is composed of three uni-axial accelerometers and one omnidirectional hydrophone. In this experiment, communication signals were generated by a source positioned at sea-floor (104m local depth). The VSA was placed about 40m below the sea surface.

In order to simulate the MakaiEx underwater channel replicas, the Ocean Acoustic and Seismic Exploration Synthesis (OASES) numerical model was used. OASES can calculate the horizontal and vertical particle velocities. The present work uses the pulse (OASP) and transmission loss (OAST) modules.⁷

A. UNDERWATER SCENARIO

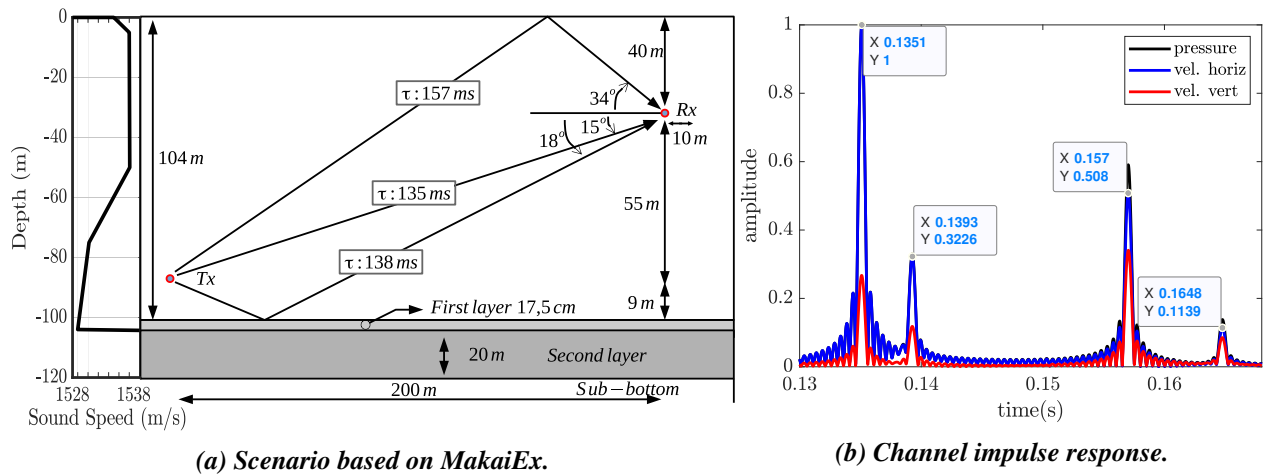


Figure 3: Underwater scenario and channel impulse response.

Figure 3 presents the underwater scenario and the normalized channel impulse response (CIR). The sound speed profile is represented on the left of Fig. 3a. This profile was measured during MakaiEx. The source (T_x) is placed at 95m depth and it is considered fixed at the seabed. Two layers and a sub-bottom compose the seabed with geoaoustic properties shown in Table 1.

For the simulation, the VS is placed at the 200m range and 40m depth. Moreover, a range displacement is made in order to study the range variation impact on the performance. Figure 3a also presents the ray path

geometrical estimation and their arrival delays based on the source image method.¹⁵ Since the propagation model provides only a 2D estimation, the azimuth angle θ_0 is considered 0° in Eq. 6.

The bottom parameters were estimated and they are shown in Table 1.¹⁶ This table shows the density ρ , the compressional wave speed c_p , shear wave speed c_s , compressional wave attenuation α_p , and the shear attenuation α_s , for each layer.

Figure 3b shows the VS CIR (pressure and particle velocities) for a reduced time. In Fig. 3b the pressure amplitude is normalized by the maximum value. The particle velocities are normalized by the maximum between horizontal and vertical components. The horizontal particle velocity has a similar amplitude attenuation than the pressure channel. On the other hand, the vertical particle velocity surface reflection (3^{rd} arrival) presents more energy than the direct path (1^{st} arrival). This is indicative of the vertical particle velocity sensitivity to surface and bottom reflections.

Table 1: MakaiEx bottom characteristic used in the OASES.¹⁶

Layer	Thickness(m)	$\rho(\text{g/cm}^3)$	$c_p(\text{m/s})$	$c_s(\text{m/s})$	$\alpha_p(\text{dB}/\lambda)$	$\alpha_s(\text{dB}/\lambda)$
First	0.175	1.6	1570	67	0.6	1.0
Second	20	2.1	1700	700	0.1	0.2
Sub	...	2.1	2330	1000	0.1	0.2

B. COMMUNICATION SETUP

The simulated message is a random series of N symbols (Table 2). The N symbols are composed of the training sequence (N_t) and the payload of N_r symbols (running symbols). The carrier frequency is 12kHz and the sampling frequency is 48 kHz. Simulations use Binary Phase-Shift Keying (BPSK) and 4-PSK. The symbol rate for 4-PSK is 187.5 bits/s, while for the BPSK, the symbol rate reaches 750 bits/s. These symbol rates were chosen based on the channel impulse response (see Fig. 3b), which presents four strong arrivals during 5 ms. The number of symbols to train the equalizer, and the number of feedback and feed-forward taps were empirically set to a suitable convergence of the MSE.

Table 2: Communication parameters.

Parameters	Description	Value
Modulation	PSK	BPSK / 4-PSK
f_s	sample rate	48000 Hz
f_0	carrier frequency	12000 Hz
R	symbol rate	187.5-750 bit/s
N_t	training symbols	1000 symbols
N_r	running symbols	1000-100000 symbols
L	CIR time	≈ 340 ms
N_1	feed-forward DFE span	15 symbols
N_2	feedback DFE span	10 symbols

4. RESULTS AND ANALYSES

This section quantifies the performance of vector sensors in communication systems. First, the simulation results show the effect of particle velocities in the transmission loss. Then, the VS beam steering performance is analyzed using the vertical and horizontal particle velocity individually and jointly. At last, a comparison among VS beam steering and VS passive time-reversal intends to show the capability of inter-symbol interference mitigation when VS is used.

A. ACOUSTIC PROPAGATION

Transmission Loss (TL) is commonly used to indicate how the signal decreases in intensity with range and depth. It is also used to determine interference caused by the surface and bottom reflections. Figure 4 shows the pressure channel TL. The sound speed profile in the lower half of the water column is downward refracting. This condition results in a convergence zone at approximately 80 m depth.

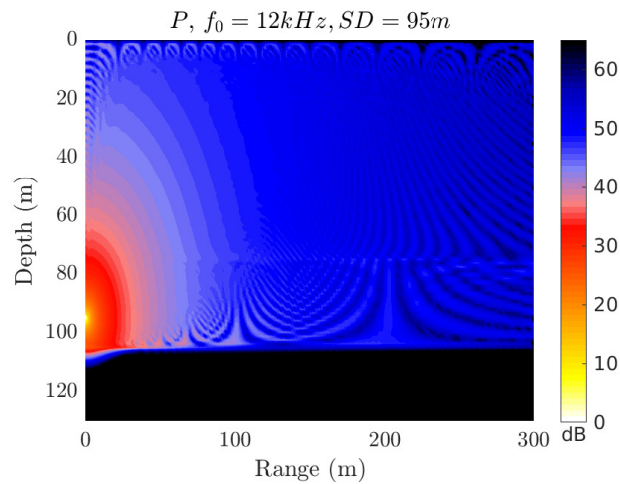


Figure 4: Transmission Loss for the pressure sensor.

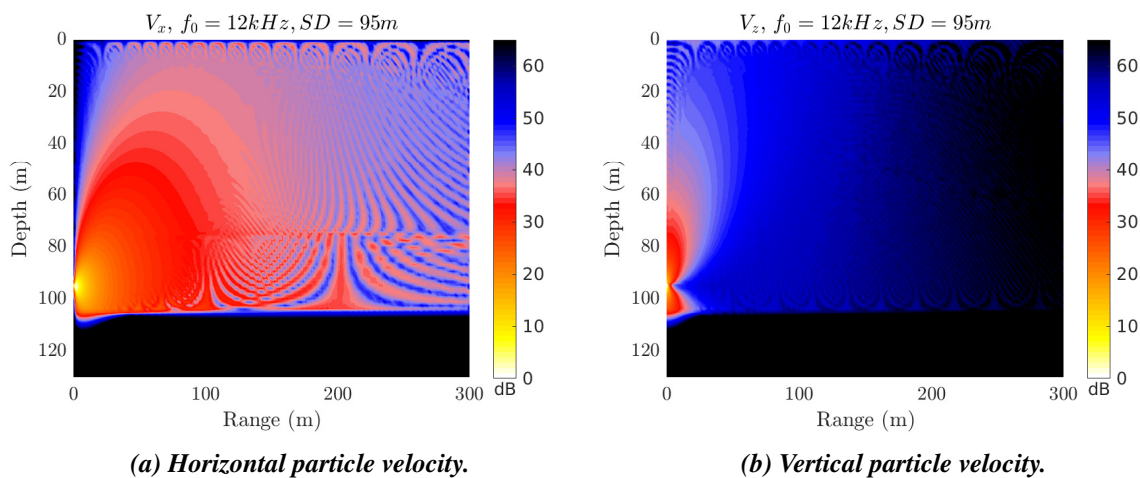


Figure 5: Transmission Loss for particle velocity.

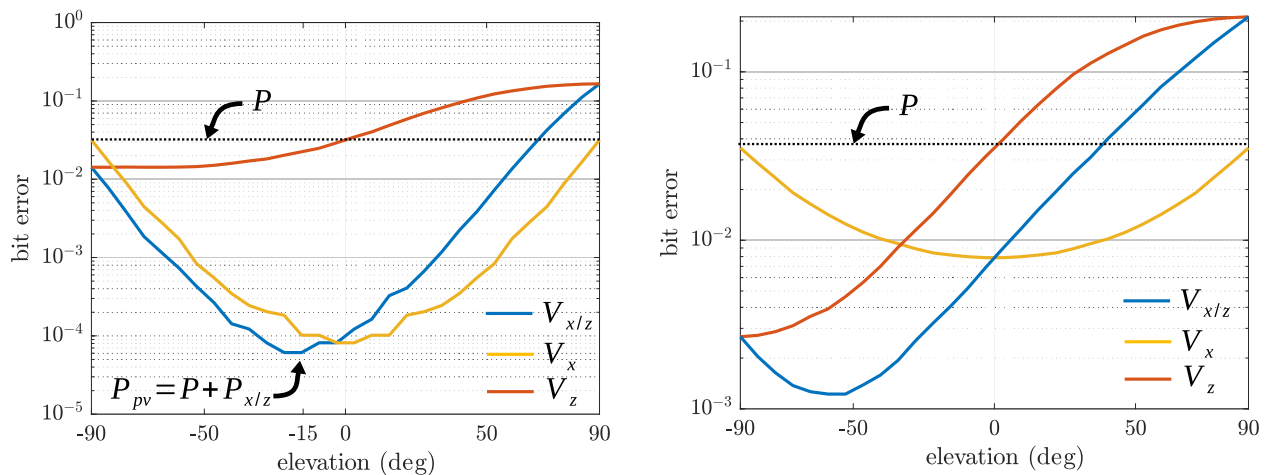
The horizontal and vertical particle velocities TL are represented in Fig. 5. For the horizontal particle

velocity TL (Fig.5a), the attenuation along range is smaller than for the pressure field. The convergence zone at 80 m depth is amplified compared to the pressure field. Furthermore, constructive and destructive interferences are noticed around the receiver position, which may influence the performance in range. On the other side, the vertical particle velocity TL (Fig.5b) shows a severe attenuation in range. As a result, the vertical component of particle velocity will only contribute meaningfully relatively close to the source (or high SNR).

In summary, the TL figures indicate that the energy is more concentrated on the horizontal axis. The interference is more evident in the pressure and horizontal particle velocity fields. Moreover, the vertical particle velocity has higher attenuation in range than pressure and horizontal particle velocity.

B. VECTOR SENSOR BEAM STEERING

Vector sensor beam steering is a method that weights the particle velocity components resulting in a steered angle. The individual channels analysis is proposed in order to understand how each particle velocity axis impacts the performance. Thus, if V_x or V_z is set to zero in Eq. 6 (2D), each particle velocity component can be analyzed individually.



(a) BER versus elevation for free-field isovelocity, SNR=4dB, 4-PSK.

(b) BER versus elevation for the proposed scenario, SNR=10dB, BPSK.

Figure 6: VS beam steering. Individual channel analysis.

Figure 6 shows the effects of each particle velocity component and their combination in the bit error performance. Figure 6a shows the result simplifying the proposed scenario for isovelocity and free-field conditions (removing the boundaries). The horizontal particle velocity effect in the bit error is seen by the V_x curve. This curve presents the worst bit error performance for $\pm 90^\circ$, which is equivalent to the pressure-only usage. The best bit error performance is achieved at 0° by summing the horizontal particle velocity to the pressure. Figure 6a also presents the vertical component analysis (V_z). For this component, the best performance is achieved at -90° (where -90° is the bottom direction). However, note that the impact of this component on the performance is small.

Figure 6a shows that V_x (at 0°) presents better performance than V_z (at -90°), individually. However, their combination further improves the bit error performance, which shows that the best performance is achieved at -15° (source direction). This is an expected result due to the directional gain to the source direction (intrinsic SNR improvement).

Figure 6b also shows the individual channel analysis, except that the original scenario presented in Fig. 3a is used. While the lowest bit error was achieved pointing toward to the source for the free-field

scenario, Fig. 6b shows that the best performance is found for angles of approximately -60° . This result can be explained looking at each particle component individually. In this figure, the vertical particle velocity (at -90°) outperforms the horizontal component (at 0°). This result indicates that the vertical component has more impact on the combined result than the horizontal one. Hence, these results indicate that particle velocities can be used for both SNR improvement and ISI mitigation (in a multipath environment).

Although the vertical component brings an advantage for the performance, this channel presents severe attenuation (see Fig. 5b). Thus, its impact on performance depends on the SNR. Figure 7 shows the combined results for discrete SNR values. The dashed line is the minimum value curve of the bit error for each SNR. This curve indicates that the optimum angle varies from the source direction (-15°) to -75° . That supports this idea that steering to the source direction could result in better performance (assuming the direct path as the most energetic path). However, this relation is only guaranteed in the free-field environment. Figure 7 shows that, in a multipath environment (and non-isovelocity sound speed profile), the angle that results in the best performance may not relate to the source direction. Considering that communication issues can be seen as ISI or SNR problems, the result is related to ISI.

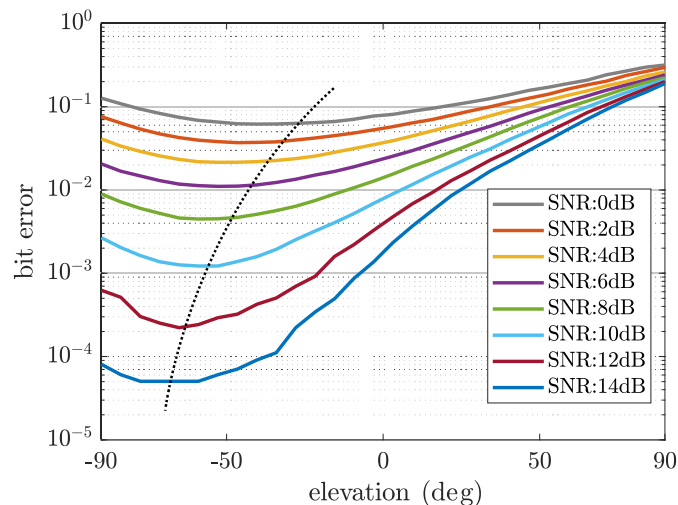


Figure 7: BER versus elevation. Combined results for SNR values, BPSK.

C. COMPARATIVE ANALYSIS

The VS beam steering method quantified in the previous section shows that there is an “optimum” angle that results in the lowest bit error. In this section, the VS beam steering (VS-bs) is compared to VS passive time-reversal (VS-ptr) via bit error analysis versus SNR and range.

Figure 8 shows the comparative analysis between VS-bs and VS-ptr. The pressure-only sensor performance followed by a DFE is also shown for reference (p-ch1). For this comparative analysis, VS-bs has a fixed angle set at -50° . In Fig. 8a, VS-bs needs 7dB to achieve 10^{-3} of error, which is 1.5dB lower than VS-ptr and 9dB lower than p-ch1. Thus, the result shows the performance advantage provided by VS, which reinforces the ISI capability of VS. Furthermore, for the proposed scenario, VS-bs shows better performance than VS-ptr, especially for higher SNR values.

The performance is also quantified by varying the receiver range for a given SNR. Figure 8b shows the bit error along 10m for a SNR value equal to 4dB. It is noted the oscillatory behavior, where the bit error performance varies from 0.05 to 0.008. This pattern may be related to the constructive and destructive interference along distance showed on the TL figures. VS-bs shows the lowest bit error at most ranges, even for a fixed angle value along with the range, which may not be the “optimum” angle.

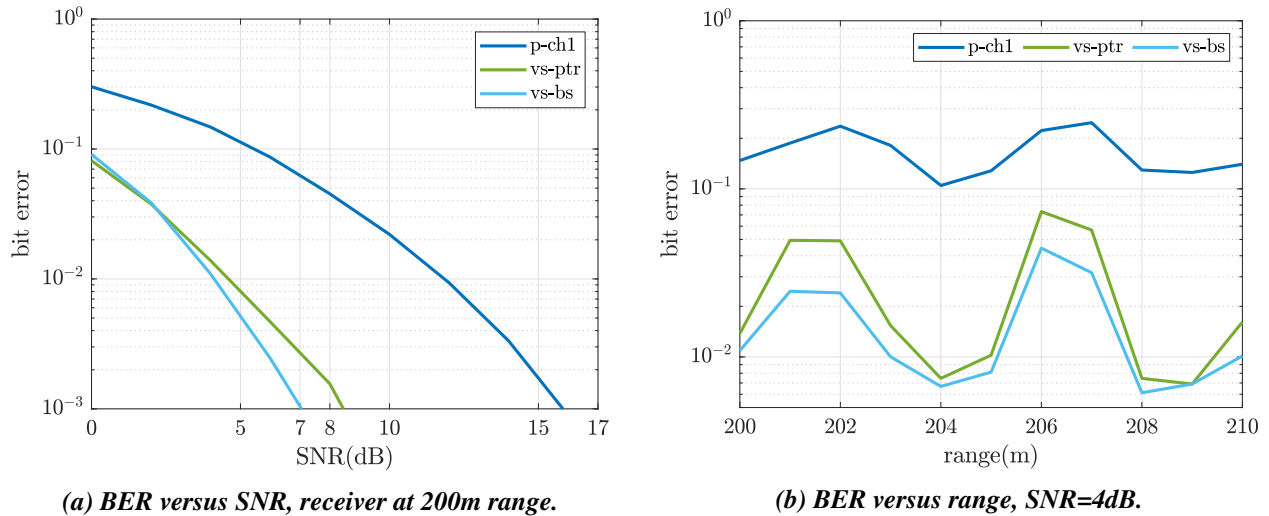


Figure 8: Comparative analysis, 4-PSK.

Thus, the comparative analysis shows that VS-bs provides better performance than VS-ptr. It was seen that for SNR values lower than 4dB the performance between methods is similar, while for higher values the VS-bs outperforms VS-ptr. The performance along range also showed that VS-bs still present the best performance even the fixed chosen angle may not be optimum.

5. CONCLUSION

The present work quantifies the vector sensors performance for a point-to-point communication system. First, the simulation results show the particle velocity effect in the transmission loss. The interference along range and the vertical particle velocity attenuation were noticed. These effects aided to explain the variability in range and the vertical component impact in the communication performance. Then, the VS beam steering method was analyzed using the vertical and horizontal particle velocity individually. This method takes advantage of the particle velocity information weighting the velocity components, which is equivalent to steer the angle to an optimum direction (lowest bit error). The individual channel analysis helped to understand that the best performance may not be related to the source direction. At last, a comparison among VS beam steering, VS passive time-reversal, and a pressure-only sensor intended to show the VS beam steering spatial filtering capability in a simple and straightforward method.

These initial results showed the VS ISI mitigation capability. Although restricted to the proposed scenario, the individual channel analysis, and the comparative analysis are tools that tried to link the acoustic particle motion physics to the results. In this sense, this analysis provides another possibility to quantify and explain the VS capability for communications usage.

ACKNOWLEDGMENTS

This work was partially funded by the Postgraduate Study Abroad Program of the Brazilian Navy, Grant No. Port. 227/MB/2019.

REFERENCES

- ¹ M. Chitre, S. Shahabudeen, and M. Stojanovic, "Underwater Acoustic Communications and Networking: Recent Advances and Future Challenges," *Marine Technology Society Journal*, vol. 42, pp. 103–116, Mar. 2008.
- ² A. Abdi, H. Guo, and P. Sutthiwan, "A New Vector Sensor Receiver for Underwater Acoustic Communication," in *OCEANS 2007*, (Vancouver, BC), pp. 1–10, IEEE, Sept. 2007. ISSN: 0197-7385.
- ³ C. H. Sherman and J. L. Butler, *Transducers and arrays for underwater sound*. Monograph series in underwater acoustics, New York: Springer, 2007.
- ⁴ P. Felisberto, P. Santos, and S. M. Jesus, "Acoustic Pressure and Particle Velocity for Spatial Filtering of Bottom Arrivals," *IEEE Journal of Oceanic Engineering*, vol. 44, pp. 179–192, Jan. 2019.
- ⁵ M. Hawkes and A. Nehorai, "Surface-mounted acoustic vector-sensor array processing," in *1996 IEEE International Conference on Acoustics, Speech, and Signal Processing Conference Proceedings*, vol. 6, (Atlanta, GA, USA), pp. 3169–3172, IEEE, 1996.
- ⁶ L. E. Kinsler, ed., *Fundamentals of acoustics*. New York: Wiley, 4th ed., 2000.
- ⁷ H. Schmidt, "OASES - User guide and reference manual," manual, Department of Ocean Engineering Massachusetts Institute of Technology, Oct. 2019.
- ⁸ M. Hawkes and A. Nehorai, "Acoustic vector-sensor correlations in ambient noise," *IEEE Journal of Oceanic Engineering*, vol. 26, pp. 337–347, July 2001.
- ⁹ T. Gabrielson, "Design Problems and Limitations in Vector Sensors," proceedings of the Workshop on Directional Acoustic Sensors, Naval Undersea Warfare Center Division and Office of Naval Research, Newport, Rhode Island, Apr. 2001.
- ¹⁰ M. Stojanovic, "Recent advances in high-speed underwater acoustic communications," *IEEE Journal of Oceanic Engineering*, vol. 21, pp. 125–136, Apr. 1996.
- ¹¹ A. Song, M. Badiy, P. Hursky, and A. Abdi, "Time reversal receivers for underwater acoustic communication using vector sensors," in *OCEANS 2008*, (Quebec City, QC, Canada), pp. 1–10, IEEE, Sept. 2008.
- ¹² W. A. Kuperman, W. S. Hodgkiss, H. C. Song, T. Akal, C. Ferla, and D. R. Jackson, "Phase conjugation in the ocean: Experimental demonstration of an acoustic time-reversal mirror," *The Journal of the Acoustical Society of America*, vol. 103, pp. 25–40, Jan. 1998.
- ¹³ J. G. Proakis and M. Salehi, *Digital communications*. Boston: McGraw-Hill, 5th ed., 2008.
- ¹⁴ M. Porter, B. Abraham, M. Badiy, M. Buckingham, T. Folegot, P. Hursky, S. Jesus, B. Kraft, V. McDonald, and W. Yang, "The Makai Experiment: High-Frequency Acoustics," in *ECUA*, (Carvoeiro, Portugal), p. 10, June 2006.
- ¹⁵ P. Felisberto, O. Rodriguez, P. Santos, E. Ey, and S. Jesus, "Experimental Results of Underwater Cooperative Source Localization Using a Single Acoustic Vector Sensor," *Sensors*, vol. 13, pp. 8856–8878, July 2013.

- ¹⁶ P. Santos, O. C. Rodríguez, P. Felisberto, and S. M. Jesus, “Seabed geoacoustic characterization with a vector sensor array,” *The Journal of the Acoustical Society of America*, vol. 128, pp. 2652–2663, Nov. 2010.